

# Department of Electrical and Computer Systems Engineering

## Technical Report MECSE-31-2004

A SIMULINK Model for Simulation of Optical Communication  
Systems: Part I –Single Channel Transmission

LN Binh and Jay Armstrong

**MONASH**  
**UNIVERSITY**

# A SIMULINK MODEL FOR SIMULATION OF OPTICAL COMMUNICATIONS SYSTEMS: PART I – SINGLE-CHANNEL TRANSMISSION

L.N. Binh and Jay Armstrong

Department of Electrical and Computer Systems Engineering, Monash university, Clayton

Victoria 3168 Australia, e-mail: [le.nguyen.binh@eng.monash.edu.au](mailto:le.nguyen.binh@eng.monash.edu.au)

## **Abstract**

*Optical communications have advanced tremendously over the last two decades, especially when optical amplifiers were invented in the late 80s. Advances in optical communications systems have been demonstrated in practice including a number of commercialised simulation packages. However no complete simulation package has been developed under MATLAB Simulink platform that are readily available and popular in engineering systems, especially as a teaching tool. This report aims to investigate the various issues currently plaguing physical implementation of optical transmission systems utilizing super dense channel spacing (SDWDM) at a bit rate approaching 40 Gb/s under the SIMULINK optical simulator, for advanced optical communications systems. Dispersion and carrier chirp effects are explored. The benefits of a chirped transmission system have also been exploited. Signal propagation through  $n$  external optical modulator, the optical fiber. Based in the MATLAB Simulink, the simulator simplifies the simulation blocks of advanced optical transmission system.*

## *TABLE OF CONTENTS*

1	INTRODUCTION .....	3
2	Overview of System Components .....	4
2.1	Receiver Noise Sensitivity:.....	4
2.2	Optical fibers .....	4
2.3	Optical Transmitters .....	5
2.4	Dispersion.....	6
2.5	Polarization Mode Dispersion .....	7
2.6	Carrier Chirp.....	8
2.7	The Mach Zehnder Interferometric Modulator.....	8
2.8	Data Sampling .....	11
3	THE SIMULINK <sup>®</sup> SIMULATOR.....	11
3.1	Assumptions .....	13
3.2	Data sampling .....	14
3.3	The carrier.....	14
3.4	Data pulses.....	15
3.5	Equipment.....	15
3.6	System Initialization .....	16
3.7	Generating data streams and carriers .....	16
3.8	The data random-bit-pattern pulse trains .....	17
3.9	Carrier Modulation .....	17
3.10	The split step propagation model.....	20
3.11	Dispersion as a Low Pass Filter.....	24
3.12	The linear delay .....	25
3.13	PMD as a Filter.....	27
3.14	Non-Linear Operator .....	28
4	The Simulator and a Case Study.....	32
5	CONCLUDING REMARKS.....	42
6	References.....	44
7	APPENDIX.....	45

## *TABLE OF FIGURES*

Figure 1:	SIMULINK Block Diagram of the Simulator .....	12
Figure 2:	Data Stream block sub system.....	19
Figure 3	The Fibre split step Fourier propagation model .....	22
Figure 4:	Plot of the fibre delay term as a function of $u$ .....	26
Figure 5:	Non-linear effects model .....	31
Figure 6 :	Initializing the simulator .....	34
Figure 7:	Sample screen shot of the SIMULINK simulator.....	34
Figure 8:	(a)-(e) 5mW simulation – Non-linear effects negligible, $N=1$ .....	39
Figure 9:	50mW case – Non-linear effects, $N=0.429$ .....	41
Figure 10:	Comparison of modulator output and fiber outputs for an input power of 5mW .....	42

# 1 INTRODUCTION

Over the last twenty years it has been witnessed the realization of low cost, low loss optical fibers. Superior information capacity and versatility has seen optical fibers become the preferred medium for modern long-haul ultra-high speed communication systems [1] However, the ever-constant desire to increase data transmission rates requires further research to fulfill the potential of fiber optic systems, in particular the flexibility of upgrading a particular wavelength channel from 10 Gb/s, say to 40 Gb/s.

As material developments plateau, focus shifts from materials to transmission properties; a desire to understand the propagation effect of fiber optics, as well as the transmission characteristics of optical signals. It is anticipated that optimizing the various linear and non-linear effects present in modern optical transmission systems and their optical-electrical (O/E) components would lead to further developments in data transmission rates. This report aims to develop and simplify the optical transmission system. Of particular interest were the effects of dispersion and polarisation mode dispersion, the two single critical effects limiting the optical data transmission rates[2]. This work has led to the development of a visual based, modeling platform, using MATLAB Simulink. This platform models signal propagation through a modern optical transmission system with the modeling of the fiber propagation through the split step method. It is anticipated that this platform will be a valuable tool for further research into different optical systems This understanding can in turn be applied to optimize the performance of systems already being installed. Through detailed research into physical limitations, means of measuring and optimizing systems will become apparent. In particular this work aims to investigate the various issues currently plaguing physical implementation of optical transmission systems operating of the super dense WDM (SDWDM) at transmission rate in excess of 40Gb/s.

## 2 Overview of System Components

In general an optical communications would consist of optical sources and modulators, multiplexers, fiber, receivers and transmitters. The following sections outline the major components of a general optical transmission system. An explanation of their operation is given as well as their role within a simulator. Various limiting parameters associated with each photonic or optoelectronic device are also introduced.

### 2.1 Receiver Noise Sensitivity:

Initially receivers were considered and in particular the effects of noise relative to their sensitivity. It is determined that the noises accumulated in photo-detectors are of three distinct types: (i) Laser intensity noise: Primarily caused due to spontaneous light emissions occurring in the transmitter. (ii) Thermal noise: A result of connecting electronic components to the receiver. (iii) Photonic quantum shot noise: a result of the quantum nature of photons.

Thermal noise can be reduced if the transfer impedance can be increased, but this would reduce its effective bandwidth. Essentially low noise amplifiers are connected to the photo diode, if a narrow bandwidth amplifier then only a few decibels (dB) of noise should be present. Middle bandwidth amplifiers would incorporate about 6-8dB of noise, and high frequency amplifiers should cause less than 15dB of noise. Shot noise is simply reduced by reducing the intensity of the light that is transmitted. Similarly, applying various filters will limit reflections back into the laser source and reduce laser intensity noise. As receiver noise is controllable through already known methods [[2][16]] but it is not a major focus of this paper.

### 2.2 Optical fibers

Apparently named single mode fibers (SMF), they are designed so as to maintain an optical signal integrity for as long as possible. This gives single mode fibers incredible data capacity at

very low losses, lending them too many various applications. As a result, the standard SMF (ITU G.652) have become the primary means through which data is transmitted. Further advanced optical fibres can also be used such as NZ-DSF, Corning LEAF etc. with large effective index area to maximize the channel input optical power. The dispersion of the transmission medium can also be compensated using various dispersion compensating or management schemes.

### **2.3 Optical Transmitters**

In designing any fiber optic system one must decide how the electrical data signal can be converted into an optical bit stream. For a system designer a number of options exist. Usually, the output of an optical source, such as a semiconductor laser, is modulated through the application of an electrical signal. Direct application of this current to control the laser gives rise to the term direct modulation; conversely external modulation utilizes a separate photonic device, such as the Mach-Zhender Interferometric modulator (MZIM), to control the optical intensity pulse output. This gives rise to the two modulation formats, non-return to zero (NRZ) and return to zero (RZ). If the RZ method is used, then the optical pulse used to represent one bit is shorter than the allocated time slot for the bit, also known as the bit duration.

Before the completion of the bit duration the optical pulse returns to its zero value. In the NRZ format the pulse does not automatically return to zero. Rather the optical pulse remains on until the end of the bit duration. This means that the pulse widths in a NRZ format can vary according to the bit stream being transmitted. On/off transitions occur less regularly in the NRZ format therefore reducing the bandwidth associated with a particular bit stream. This is usually by a factor of about two. This smaller bandwidth leads to NRZ often being the format of choice in data transmission systems.

The optical carrier waveform generated by a CW operating laser source before modulation is usually represented by:

$$C(t)=A \cos(\omega_0 t+\phi) \quad (eq. 1)$$

where  $A$  is the amplitude of the optical signal envelop,  $\omega_0$  is the carrier frequency and  $\phi$  is the carrier phase [1][16] Any of these parameters can be used as variables for modulating electrical signal to optical domain. The MZIM as illustrated later utilizes a phase shift to induce amplitude modulation.

## 2.4 Dispersion

In IM/DD systems, usually operating at less than 2.5 Gb/s, the dispersion had not been a major issue owing to the rather widely spaced channels used. However for higher bit-rate systems (>10 Gb/s) incorporating DWDM require an increased density in channel spacing. As a result dispersion has become a very important issue. This causes inter-symbol interference at the receiver increasing bit-error rates (BER), eventually rendering the signal unrecognizable. Figure 4 illustrates this dispersion issue and the occurrence of cross talk in faster systems utilizing DWDM.

Chromatic dispersion is defined as being the spreading/broadening of transmitted data pulses as a function of the group velocity of different optical frequencies. In advanced systems employing multiplexed channel and narrow channel spacing, the compensation method would not sufficiently overcome the problem of dispersion. In fact dispersion effects have come to be the single biggest limiting factor in such ultra-long reach optical communications systems. The effects of dispersion are directly related to the speed of transmission. Thus ultra-high speed systems are more greatly affected by dispersion that occurs as a result of two major factors: (i) Different wavelengths in DWDM systems: channel transmission utilizes different wavelengths to send data. This causes slight variations in the refractive index of optic fiber causing signal dispersion; and (ii) The transmitter: ‘chirp’ induced by the laser modulator will cause dispersion by slightly varying the carrier frequency, altering the refractive index of the fiber.

If  $\Delta\omega$  represents the spectral width of an optical pulse it can be shown that the pulse dispersion over a length of fiber  $L$  is given by:

$$\Delta T = L\beta_2\Delta\omega \quad (eq. 2)$$

where  $\beta_2$  is known as the GVD parameter. It is this parameter that primarily determines the broadening of a pulse as it propagates through an optical fiber. Sometimes ((eq. 2) can be rewritten to consider the range of wavelengths that are emitted by the optical source. Defined as dispersion this relation is given by:

$$D = -2\pi c\beta_2/\lambda^2 \quad (eq. 3)$$

where the dispersion is expressed in ps/nm.km,  $\lambda$  is the light wavelength and  $c$  is the speed of light. Both of the aforementioned causes were considered before it was decided to focus on the ‘chirp’ effect. This was directly related on the desire to optimize current systems rather than attempt to generate a whole new means of transmission.

## 2.5 Polarization Mode Dispersion

Practical optical fibers are inherently asymmetric on account of the non-perfect conditions of their drawing. As a result, light waves in one polarization axis can move at different speeds to those in the other polarization axis. The effects of this delay become more critical at faster transmission speeds. The varying speed causes delay in transmitted pulses. At higher transmission rates this can cause signals to overlap, becoming indistinguishable at the receiver.

To quantify this occurrence the differential group delay (DGD) is defined as  $\Delta\tau$ . Existing statistical models make use of a Maxwellian distribution for the consideration of PMD effects.

From the statistical relationship a mean value can be determined and is used to quantify a fiber’s PMD. This is represented by  $\delta\tau$  and measured in units of ps/ $\sqrt{\text{km}}$ . [[15],[7]

## 2.6 Carrier Chirp

With chirp found to be a major player in the cause of dispersion this parameter became a focus for the project. If the chirp induced by the system transmitter could be minimized then so to might the dispersion and thus the overall system performance. To achieve these goal two areas need to be considered. Firstly the chirp causes impairments to other parameters in an optical transmission system. Secondly, the actual mechanism of signal transmission, that is the modulator. This paper will focus on the Mach-Zehnder interferometric modulator on account of its regular use in industry and its presence in the university optics laboratory. It was the developed understanding of the chirp parameter and its effects on system performance that led to the decision to simulate a modern fiber optic system using Simulink and will be discussed in greater detail in later stages of this writing.

## 2.7 The Mach Zehnder Interferometric Modulator

As previously mentioned dispersion was determined to be the major limiting factor in optical systems. Further to this point it was found that the single biggest contributing factor to signal dispersion was transmitter chirp. Paramount to an understanding of chirp is a need to understand the technical operation of the system transmitter. This paper focuses on the Mach-Zehnder Interferometric Modulator (MZIM) on account of its popular use in practical systems.

The MZIM is a device that uses double side-band amplitude modulation (DSB AM) to transmit data as a stream of optical pulses. It is an externally modulating system ideally suited to high-speed data transmission on account of its narrow line-width. Figure 6 illustrates the topology of a MZIM. It should be noted that figure 6 depicts a single electrode model. Also available is a dual electrode device but the principles behind its operation remaining the same. This paper focuses primarily on the single arm model.

The MZIM makes use of a titanium diffused LiNbO<sub>3</sub> wave-guide in an interferometric configuration. By applying an external voltage the refractive index of electro-optic materials can change. This can be used to alter the phase of one of the optical paths. When the two paths merge at the output of the modulator the two waveforms interfere with one another. In the absence of a voltage, that is in the ‘On state.’ The phase of both carriers is equal, thus as they emerge from the modulator constructive interference occurs generating a signal. In the ‘Off state’ a voltage is applied to the electro-optical material, in this case LiNbO<sub>3</sub>. This causes modulation to the carrier in the modulated guide, changing its phase. A change of 180 degrees in phase will cause destructive interference that will cancel the two carriers as they recombine. This eradicates the waves generating an ‘off’ signal [8][9][10][11][12][13][14]. Thus, by driving the electrode by the data stream to be transmitted one can control whether constructive or destructive interference occurs allowing the electronic data stream to be converted into an optical signal. Unfortunately, it is not possible to instantly change the phase delay of the modulator arms, which leads to the occurrence of chirp. Rather the phase delay generated by the electrode changes transiently. Thus the chirp for the single electrode MZIM can be found from the output electric field of the MZIM. The output electric field of the lightwaves is given as

$$E_0 = \frac{E_1}{2} \{ e^{j\theta_1} + \tau e^{j\theta_2} \} \quad (\text{eq. 4})$$

where  $\phi_1$  and  $\phi_2$  represent the phase changes in arms 1 and 2 respectively.  $\tau$  is a scaling factor between 1 and 0 accounting for the particular geometry of the device being analyzed. A value less than 1 denoting a power split not 50/50 between the two arms can be found from:

$$\tau = \frac{(\epsilon^{1/2} - 1)}{(\epsilon^{1/2} + 1)} \quad (\text{eq. 5})$$

Where  $\varepsilon$  is the extinction ratio of the device, the ratio power of a '1' to a '0.' The chirp, often denoted by the parameter  $\alpha$ , is defined by

$$\alpha = \frac{2I \left( \frac{d\phi}{dt} \right)}{\frac{dI}{dt}} \quad (\text{eq. 6})$$

where,  $\phi$  is the instantaneous phase of the optical signal and  $t$  is time. It is the instantaneous optical signal intensity and found using:

$$I = \frac{E_i^2}{4} \left\{ 1 + \tau^2 + 2\tau \cos(\phi_1 + \phi_2) \right\} \quad (\text{eq. 7})$$

where  $\phi$  is defined as:

$$\phi = \tan^{-1} \left\{ \frac{\sin \phi_1 + \tau \sin \phi_2}{\cos \phi_1 + \tau \cos \phi_2} \right\} \quad (\text{eq. 8})$$

Thus the chirp is directly related to the rate of change of the phase of the modulator arm.

Substituting into (eq. 7) redefines the modulator chirp as:

$$\alpha = \frac{\phi_1 + \tau \phi_2 + \tau(\phi_1' + \phi_2')}{-\tau(\phi_1' - \phi_2') \sin(\phi_1 - \phi_2)} \quad (\text{eq. 9})$$

where ' denotes a time derivative. Further substitution for  $\phi$ , as defined by (eq. 8) gives:

$$\alpha = \frac{V_1 + \tau^2 V_2 + \tau(V_1 + V_2) \cos\{\eta(V_1 - V_2) \sin \omega t - \eta V_b\}}{\tau(V_1 - V_2) \sin\{\eta(V_1 - V_2) \sin \omega t - \eta V_b\}} \quad (\text{eq. 10})$$

The (eq. 9) gives the chirp in terms of a specific bias voltage, as defined by the operator, and driven by a sinusoidal carrier frequency with angular frequency  $\omega$ . Chirp can now be found for

the MZIM at any bias point. This will enable theoretical calculations to be performed that can be used to verify future experimental results.

From the aforementioned equations it is apparent that MZIM frequency chirp can theoretically be eliminated by ensuring the propagation constants of each arm of the modulator change at the same rate. However, this is not possible in a single electrode device as only one arm changes phase. Secondly even dual drive systems are unlikely to change at exactly the same rate meaning that in practice some degree of chirp would occur.

## 2.8 Data Sampling

With the intention of developing a discrete representation of an optical transmission system it is important to consider data sampling which is important in the simulation platform resources. Given that a deterministic signal  $s(t)$  can be represented by a set of samples taken at a sampling frequency ( $f_s$ ) that is twice that of the signal bandwidth ( $W$ ). Or mathematically:

$$f_s > 2W \text{ samples /second} \quad (\text{eq. 11})$$

The minimum value at  $f_s = 2W$  is generally classified as the Nyquist rate. To ensure that sampling errors are not introduced all data must be sampled at or above this rate. Sampling at the Nyquist rate allows the signal to be reconstructed through use of an appropriate interpolation formula. Ensuring that sampling occurs at or above the Nyquist rate would prevent undesirable signaling errors, such as aliasing.

## 3 THE SIMULINK<sup>®</sup> SIMULATOR

A simulator is designed as a platform upon which system transmission and optimization could be performed. The simulator has been developed in stages so as to minimize confusion, errors and ease of implementation. Furthermore a step by step approach allows skill sets pertaining to the simulator to be gradually developed. This section documents the simulator development,

explaining the various steps undertaken in designing the simulator as well as explaining how the components within the simulator were brought together. Coupled with the design diary this gives an accurate picture of the development of the SIMULINK prototype as shown in Figure 1.

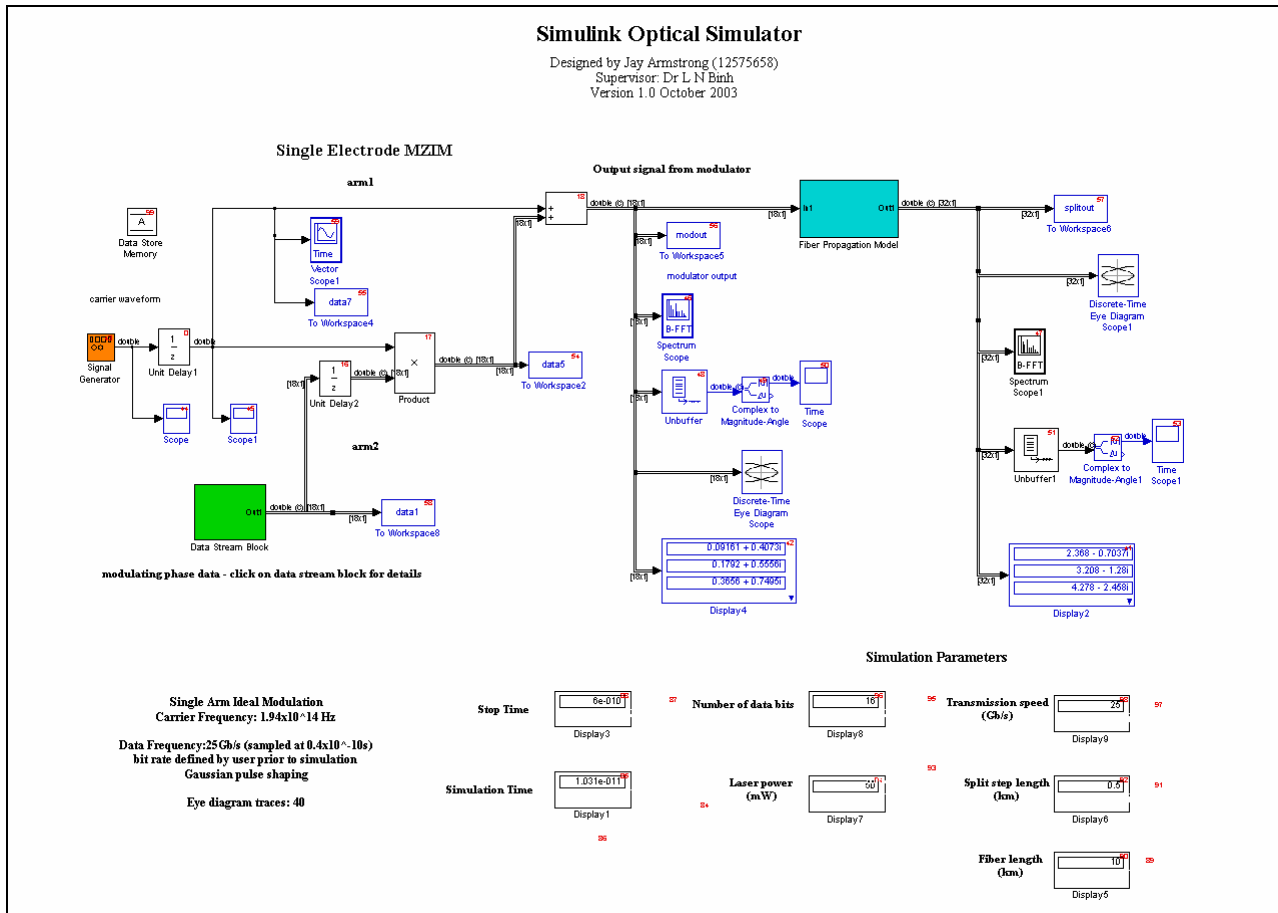


Figure 1: SIMULINK Block Diagram of the Simulator

Simulink provides a visual setup that is easier to upgrade should further research be undertaken as well as effective modeling tools. Simulink can be easier for a user unfamiliar with the programmer's methods or general programming techniques, i.e.: operators or system technicians, thereby simplifying alteration of data and settings. This reduces the likelihood of human induced error when modeling the system of choice, important in the rapidly changing area of information transmission.

Intrinsically, Simulink is a very versatile design tool. However, this also means many different factors need consideration to accurately model a system. Little experience with complex system modeling meant that a knowledge base of the system needed to be developed gradually. Owing to the complexity of the simulator prototype a number of tasks were outlined. These would simplify the design process and, pending time, allow additional tasks to be completed. The initial consideration of this paper was the dispersion parameter caused by the inclusion of modulation circuitry. Thus the primary goal of the simulator was to model system operation up to the point of data stream transmission. The simulator was broken into a number of separate stages.

The first stage consisted of the carrier generator, a data stream block to generate modulation data and the modulator model itself. Results were to be generated as eye diagrams thus allowing simple visual interpretation of results under different operating conditions. Data waveforms would also be generated to illustrate the first stages operation, outcomes and results are detailed in a subsequent section of this paper. Secondly it is the inclusion of a fiber propagation model. For random data pulses propagating along a length of fiber. To complete this secondary goal a number of small sub-models be generated with each sub-model representing a different component of the propagation effects.

### **3.1 Assumptions**

In order to design the simulator a number of assumptions are made. This section outlines those assumptions and the basis of the reasons. Some of these assumptions relate to basic issues such as software compatibility whilst others are related to the way in which data is processed during the simulator's operation. It is assumed that the simulator will be run within the Matlab program. More importantly it is assumed that the relevant **blockset** libraries have been initialised upon the users platform. This simulator was designed using Matlab 6.5 and Simulink version 5. The

specific blocksets needed to ensure operation are: (i) Simulink DSP blockset (ii) Simulink Communications Blockset

### 3.2 Data sampling

In designing the simulator a discrete rather than continuous sampling method is employed. In particular a discrete sampling system would decrease the processing power required to execute simulations and hence decrease execution time. In accordance with the sampling theorem previously outlined all data was sampled at or above the Nyquist frequency. That is all sampling was performed at twice the highest frequency within the simulator. The use of discrete sampling periods helped to ensure synchronization of the various system components as the data signal was propagated, an important consideration in optical systems. Considerations of optical transmission system parameters show the highest frequency to be that of the carrier waveform. For the purpose of this project the carrier frequency was defined as 194 THz. Thus sampling within the system needed to occur at twice this rate, approximately 400 THz in order to ensure signal aliasing issues did not arise. All blocksets requiring a discrete sampling time were given this sampling rate at which to generate data. Unfortunately this sampling rate is very high and does cause execution time to be slowed. This was deemed a necessary tradeoff to ensure accuracy.

### 3.3 The carrier

The carrier waveform is one of the most important factors within any data transmission system. For the simulator a sinusoidal carrier was assumed as

$$C(t) = A \cos(\omega_0 t + \phi) \quad (\text{eq. 12})$$

Where the carrier frequency was defined as 194 THz and the phase was set to zero. A normalised amplitude is used for simplicity. High frequency, small line-width lasers generate an oscillating

signal modeled in information transmission theory as a sinusoidal carrier. This simplifies simulations, as non-ideal waveforms can be difficult to model on existing software. As an expansion one could consider more exact carrier approximations based upon experimental data. Waveform generators could be used to model an exact practical carrier.

### **3.4 Data pulses**

Data transmission forms another critical component of the optical system simulator. For externally modulated signals the lightwave pulses are modulated with the carrier as lightwaves generated by the CW the laser sources. Two data pulses are considered: (i) for simplicity a standard return to zero (RZ) binary pulse and (ii) a RZ Gaussian binary pulse sequence. Eventually Gaussian waveform would be incorporated as it more accurately models the data waveforms generated in practical systems. The gradual rise and fall of the Gaussian pulse reflects the non-instantaneous rise/fall of modern electrical/optical equipment. If desired, the Gaussian or raised cosine or Bessel filtered pulses could be easily modified to represent NRZ by changing the Gaussian pulse period in the initialization file.

### **3.5 Equipment**

The outcome of this simulator prototype was to reflect the performance of a modern optical high speed data transmission system. Thus the simulator is modeled to reflect equipment currently used in optical data transmission systems. This would enable future experimentation to be performed in conjunction with the designed simulator. The simulator assumes an optical system comprising of a single electrode MZIM, a DFB laser source, a length of SMF-28 or NZ-DSF optical fiber, and a standard receiver system. Naturally these assumptions could be changed or expanded upon to reflect a greater variety of systems. Such expansions might include the incorporation of dispersion compensation fiber, or various amplifier and modulator setups.

### **3.6 System Initialization**

To correctly operate the simulator an initialization process is required. Written as an M-file this loads parameters and variables required for the simulator operation. Titled initialization's the user needs to run this file before starting the Simulink simulation. Failing to do so will result in an error warning. It is within the initialization file that the user can modify system parameters. The file requires a data bit rate in bits per second to be defined, a fiber length in kilometers and a split step size also in kilometers. Use of the initialization file simplifies operation for the user. All variable parameters are contained here and automatically updated in the Simulink platform upon execution. Not incorporating the initialization file would have required the user to input the same variable in multiple blocks increasing errors and complicating operation. The initialization file was deemed the simplest way to reduce errors whilst ensuring the simulator's flexibility. Apart from user-controlled parameters the initialization file includes models for the data stream waveforms. The initialization file loads the values used to model the Gaussian pulse, the carrier and determines the necessity of non-linear effects based upon the total power supplied.

### **3.7 Generating data streams and carriers**

The system transmitter could be modeled by a DFB laser carrier source and a data stream. Within its framework the Simulink platform offers a number of means for generating waveforms. Each of these was considered in turn before a final method was employed. Initially the sinusoidal source was generated in the initialization file in an attempt to give greater control over the system source. However, this complicated execution requiring longer periods of time to generate data. This led to the use of a signal generator block coupled to a discrete sampling block. This would allow a number of waveforms to be considered should the need arise, not just sinusoidal carriers. Visual confirmation was made of a sinusoidal output of the required frequency through

use of the scope block. Furthermore this block set offered easier control over waveform parameters than other considered blocks.

### **3.8 The data random-bit-pattern pulse trains**

The data pulse would be the more complicated component of the transmitter. Initially a standard string of bits was used as an input; however this seemed to limit the versatility of results that might be acquired from the simulator. Thus a random binary source was implemented. This would allow bits to be generated at a rate determined by the user in the initialization file. The Bernoulli binary generator was chosen upon recommendation by the literature contained within Simulinks help files. Assigning the initial seed parameter to a constant value this string could be held constant, for comparative purposes. Similarly varying this value would allow random strings to be generated better modeling system performance under specific conditions. This parameter is simply altered by double clicking on the block, bringing up a list of its properties.

As previously discussed the data pulses needed to be modeled as Gaussian waveforms. This would accurately reflect practical optical data generators. However the random generators offered by Simulink only generate ideal binary pulses. Thus a method for changing the ideal random pulse into a random Gaussian pulse was developed. It was deemed that a Gaussian waveform would be generated over the course of a '1' bit by multiplying that bit by a Gaussian waveform. To generate this waveform a Gaussian pulse was defined within the initialization file.

This equation can be solved for a number of points and stored. Multiplied by the randomly generated bit pulses resulted in a Gaussian waveform. Thus a '1' bit produced a waveform represented by the stored Gaussian values, whilst a '0' value resulted in no result. This set of waveforms could then be fed into the modulator model.

### **3.9 Carrier Modulation**

With both carrier and data waveforms established a model of the MZIM was required. As previously discussed, the MZIM generates a modulated data waveform through a process of constructive and destructive interference caused by a phase shift in the carrier frequency. For the simulator a single electrode MZIM is modeled. To generate the modulator model two components are required. Firstly, the geometry of the modulator needed to be taken into account. Splitting the carrier signal into two distinct components gave the two arms of the MZIM. One of these would pass untouched to the output summing device, the point at which the two arms would recombine to generate a modulated output. The second arm would model the electrode arm of the modulator. The carrier signal is passed into a multiplier and shifted by a phase shift component generated by the second of the modulator components, the modulating data stream.

For simplicity the modulating data stream was designed as a subsystem of the total transmission system, represented by the data stream block. Observation of this system is possible by double-clicking on the subsystem block.

The data stream block was the more complicated component of the transmitter model. External modulation utilizes the data to be transmitted to generate a phase shift. This is passed to the modulator and used to modulate the carrier waveform, essentially encoding the data onto the waveform. Thus the data pulse components form the input to this sub-system.

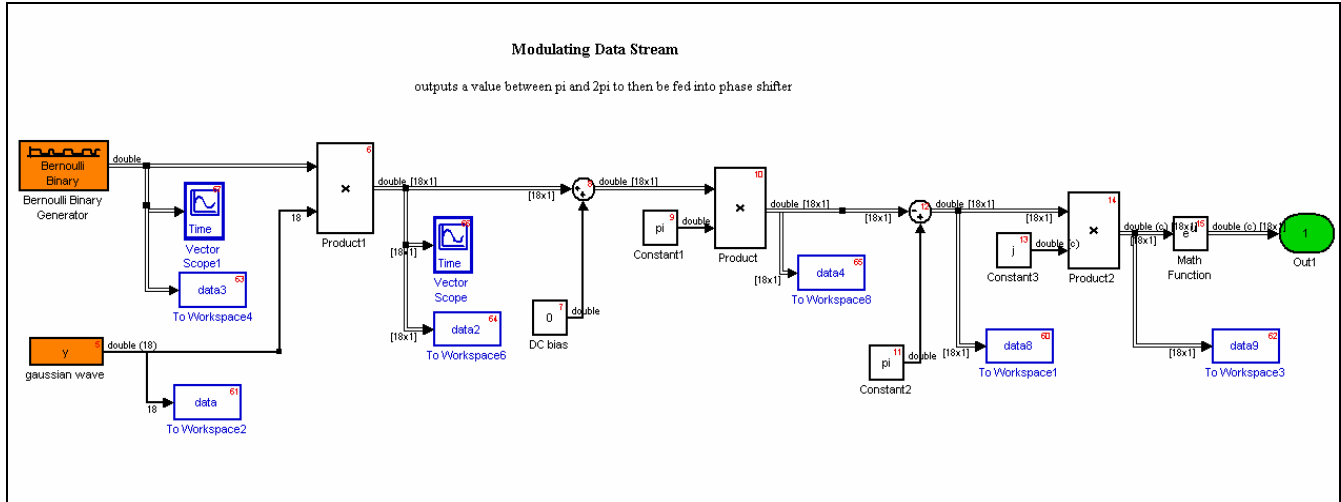


Figure 2: Data Stream block sub system

From Figure 2 it can be seen that randomly generated Gaussian pulses are first summed with a DC bias value. Next the data stream is multiplied by  $\pi$ . This converts the Gaussian pulses to a range of radian values ranging between  $\pi$ , for a '1' bit, and zero for a '0' bit. The MZIM generates a phase shift of 180 degrees between the modulator arms only if a zero is required at the modulator output. Thus the range of radian values is subtracted from a phase shift constant of  $\pi$ . This causes a zero angle to be generated for a '1' bit ( $\pi - \pi = 0$ ) and a 180 degree angle ( $\pi + \pi = 2\pi$ ) for a '0' bit. The carrier is represented by Simulink as a complex signal. To pass the correct phase shift to the electrode arm of the modulator the angular value generated in the data stream sub system must be converted to its complex notation. Thus the angle is multiplied by  $j$  and its exponential taken. This yields a phase shift represented by its complex exponential notation i.e.:  $e^{2\pi j}$ . This is then fed into the main system and multiplied by the carrier in the electrode arm of the modulator. This causes a phase shift of the carrier between 0 and 180 degrees depending on whether the data is a '0' or '1'. Summing the electrode arm to the carrier in the unmodified arm 1 causes the waveforms to cancel or complement one another thereby generating the output modulator waveform.

This is quite a complicated component of the simulator in that it required not only that the phase shift be generated accurately, but also that the data be synchronized with the carrier waveform. Synchronization was ensured using the unit delay blocks. By ensuring both blocks had the same sampling time, data was generated for every value of the carrier. Also causing complications was determining the exact way in which Simulink passed data from block to block. The format of data from each block set had to be monitored to ensure the modulating data is generating the phase shift data in a way Simulink could make use of. This is done using the signal property tool in Simulink. This states the data type at each stage of the model's execution i.e.: complex, double etc. These were double-checked by passing data to Matlab and plotting the various stages of execution. These processes will be discussed in a later part of this paper.

### **3.10 The split step propagation model**

Having designed an accurate model for the modulation of lightwaves, the propagation of these modulated lightwave channels are considered. Fiber linear and nonlinear induced dispersion effects exist over the entire length of an optical fiber. Thus differing lengths of fiber incur variable dispersion effects. Furthermore, fiber effects are not a result of one singular parameter, rather results stem from numerous parameters. As such, any attempt to model fiber propagation must take into account both the length of fiber, and the various effects that occur. Further complicating the issue of modeling is the nature of fiber effects. Some components occurring during propagation are linear in nature, others non-linear. Naturally a perfect model taking all factors into account is complicated to the point of impracticality, especially given the time frame of this project and the computer systems running this simulator. Analysis of various research papers and articles led to the adoption of the split step model [1] This method aims to consider the major effects of fiber propagation in a way that is, comparatively simpler than more precise

models. The Non-Linear Schrodinger Equation (NLSE) is regarded as the propagation equation of an optical pulse in its single mode. The NLSE is usually represented by the following equation

$$\frac{\partial A}{\partial z} + \beta_1 \frac{\partial A}{\partial t} + \frac{j}{2} \beta_2 \frac{\partial^2 A}{\partial t^2} - \frac{1}{6} \beta_3 \frac{\partial^3 A}{\partial t^3} = j\gamma |A|^2 A - \frac{\alpha}{2} A \quad (eq 13)$$

The  $\beta$  matrices correspond to the various dispersion components of the fiber. The  $\beta_1$  term represents the pure delay and representing the PMD fiber differential group delay (DGD) effects when a vector field is employed, and the chromatic dispersion represented by the  $\beta_1$  and  $\beta_2$  terms. Losses over the length of fiber are considered through the attenuation  $\alpha$  parameter, and fiber non-linearities are represented by the  $\gamma$  term. The NLSE can be used to represent the amplitude of a propagating signal in both its x and y directions. Rewriting (eq. 12) shows this propagation equation as

$$\frac{\partial A}{\partial z} + \left\{ \beta_1 \frac{\partial}{\partial t} - \frac{j}{2} \beta_2 \frac{\partial^2}{\partial z^2} - \frac{1}{6} \beta_3 \frac{\partial^3}{\partial z^3} \right\} A + \alpha A = -j \frac{\gamma}{3} \left\{ \begin{array}{l} \left( 3|A_x|^2 + 2|A_y|^2 \right) A_x \\ \left( 3|A_y|^2 + 2|A_x|^2 \right) A_y \end{array} \right\} \quad (eq. 14)$$

where  $A_x$  and  $A_y$  are the two polarized field components of the LP mode of the guided lightwaes. The split step model attempts to model various fiber effects over the length of fiber as shown in Figure 3. The model requires than the fiber segmented into a number of small sections or propagation steps, each usually represented as  $\delta z$ . Over each length of  $\delta z$  various fiber effects are assumed to act independently of one another. Each split step,  $\delta z$ , is assumed to consist of a number of discrete linear filters, each of which corresponds to a different fiber effect. The first of the filters,  $L_2^{1/2}$  is used to model the chromatic dispersion linear effects of the beam propagation.

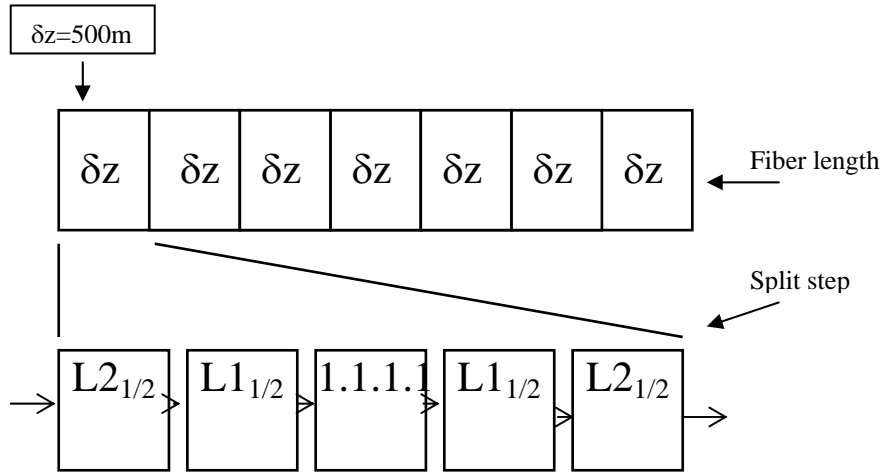


Figure 3 The Fibre split step Fourier propagation model

Another discrete filter,  $L_1^{1/2}$  is then used to model the PMD effects. These filters in turn feed the non-linear operator describing the non-linearities and attenuation through the fiber. The split step then passes back into the dispersive set of filters,  $L_1^{1/2}$  and  $L_2^{1/2}$  and operated under the inverse Fourier transform. The pulse sequence first passes into the purely linear dispersive region of the fiber, represented by the discrete filters  $L_1^{1/2}$  and  $L_2^{1/2}$ . The pulse spectrum is then convolved with that of the nonlinear operators in the frequency domain before returning to the purely dispersive region of the fiber.

Therefore, a pulse propagating through an optical fiber can be modeled by multiple iterations of the split step. In essence, the each split step can be considered as a solution to the NLSE. This solution is represented by (eq. 14).

$$A(T, z + \Delta z) \approx L_2^{1/2} L_1^{1/2} \exp \left\{ \int_z^{z+h} N(z') dz' \right\} L_1^{1/2} L_2^{1/2} A(T, z) \quad (\text{eq. 15})$$

In order to implement the split step model, a numerical solution must be made for each of the linear operators,  $L_1^{1/2}$  and  $L_2^{1/2}$ , as well as for the non-linear operator  $N$ . Parameters  $L_1^{1/2}$  and  $L_2^{1/2}$  represent the pulse propagating through a purely dispersive medium [17]. To this end, each of

these parameters can be modeled through the use of digital filters. In other words the split step can be considered a series of filter and mathematical operations mimicking the behavior exhibited by a pulse propagating through fiber. From (eq. 15)  $L_2^{1/2}$  can be found and given by

$$L_2^{1/2} = \begin{bmatrix} H_d(z) & 0 \\ 0 & H_d(z) \end{bmatrix} \quad (\text{eq. 16})$$

Within the above matrix  $H_d(z)$  can be considered to represent the time-domain filter that results in dispersion and is frequency dependent. The diagonal nature of the matrix operator  $L_2^{1/2}$  represents chromatic dispersion acting equally on both modes of propagation.

Similarly  $L_1^{1/2}$  can be defined as:

$$L_1^{1/2} = \begin{bmatrix} H_p(z) & 0 \\ 0 & 0 \end{bmatrix} \quad (\text{eq. 17})$$

Here  $H_p(z)$  represents the discrete filter in z-domain of the PMD low-pass filtering effects including its randomness with a Maxwellian distribution. As opposed to chromatic dispersion, PMD is considered to act only on one mode of propagation delay. This is due to PMD causing one mode to be delayed with respect to the other [19].

The response of any dielectric medium to light becomes non-linear, in the presence of intense electromagnetic fields. The wave-guide symmetry used to confine light to a small cross section means non-linear effects become important for long haul and ultra-high bit rate optical transmission systems[110]. In our model these nonlinear effects are included through the non-linear operator  $N$ . Non-linearities depend only on distance and as such do not requires time-domain filters in their inclusion. In essence this is a multiplier value that represents Rayleigh, Brillouin and Raman Scattering and the Kerr phase modulation occurring over the fiber length.

The bi-modal propagation equation obtained from (eq. 14) gives the non-linear operator  $N$  in its matrix form:

$$N(z') = \begin{bmatrix} -j\frac{\gamma}{3}(3|A_x|^2 + 2|A_y|^2) - j\alpha & 0 \\ 0 & -j\frac{\gamma}{3}(3|A_x|^2 + 2|A_y|^2) - j\alpha \end{bmatrix} \quad (\text{eq. 18})$$

Other nonlinear effects such as FWM, Raman scattering, modulation instability can be easily incorporated into (eq. 17) and (eq. 18) without any difficulty.

### 3.11 Dispersion as a Low Pass Filter

As signals propagating through an optical fiber it can be considered to first pass through two purely linear dispersive media. The first of these, the chromatic dispersion, is modeled using the  $L_2^{1/2}$  operator. Chromatic dispersion has no direct effect on signal amplitude; rather it causes optical signal dispersion. This means that the chromatic dispersion can be modeled through the use of an all pass filter. This means that the filter has a normalized amplitude within the Nyquist bandwidth. This bandwidth is defined by sampling theory as being twice that of the optical bandwidth. Thus, the filter is required to operate between the ranges

$$-\frac{1}{(2T_c)} \leq f \leq \frac{1}{(2T_c)} \quad [16][7],[17]$$

The group delay of such a filter is given as [112]:

$$\tau_g(\omega) = L \left[ \beta''(\omega_0) + \frac{1}{2} \beta'''(\omega_0) \Omega^2 \right] \quad (\text{eq. 19})$$

This equation consists of two terms. The first of these,  $L\beta''(\omega_0)$  represents linear delay, whilst

the second term  $\frac{L}{2}\beta'''(\omega_0)\Omega^2$  incorporates parabolic delay.

### 3.12 The linear delay

As previously stated, the linear delay is represented by,  $L^{\beta''}(\omega_0)$ . To represent this in Simulink an all pass filter is required. This will produce group delay properties that vary linearly with frequency. Rather than design such a filter from scratch, previous research was utilized [112]. This work gives a filter already capable of approximating linear delay to a high level of accuracy. This filter was given by [6][13],[7]

$$H_{lin}(z) = uv \frac{z - j\frac{1}{u}z - \frac{1}{v}}{z - juz - v} \quad (eq. 20)$$

where the parameters  $u$  and  $v$  are real numbers. In order to ensure a filter that causes phase distortion, the pole zero pair of the filter is matched. Operation over the Nyquist range defines the filter as being of unit amplitude. Thus the real number  $u$  and  $v$  can be related. This allows the filter equation to be redefined as:

$$1 = 4 \frac{u^2(1-u^2)(1-v)^3}{v(1+u^2)^3(1+v)} \quad (eq. 21)$$

The resulting filter group delay is then given by:

$$\tau_{Hlin} = \tau_0 + 2T_c^2 \frac{u(1-u)^2}{(1+u^2)^2} \quad (eq. 22)$$

within this equation the  $\tau_0$  term represents a constant common to most digital filters. However, this parameter has no effect on chromatic dispersion and can be negated and ignored. The other term contained within (eq. 21) represents the linear group delay that is needed. As this is a function of  $u$  a plot was determined to determine the range of values  $u$  can take. This was performed through the Matlab workspace. The steps used to complete this task are included in the appendices. The resulting plot of  $u$  values is shown in Figure 4.

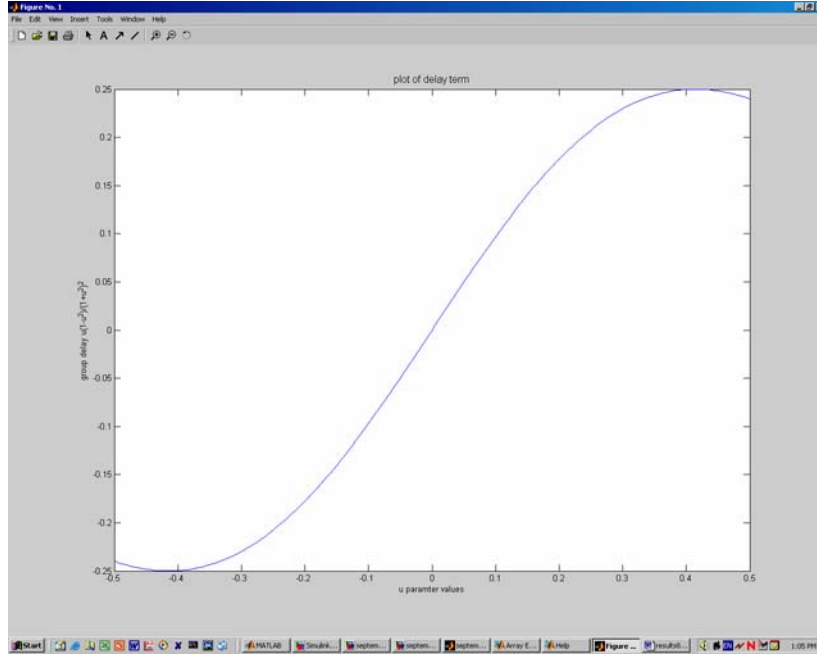


Figure 4: Plot of the fibre delay term as a function of  $u$

We note that  $u$  is limited to the range  $+0.4$ . Taking  $u$  as a maximum value and substituting into (eq. 21) shows a total linear delay of  $+0.5T_c2\Omega$ . However an error analysis shows this leads to relatively inaccurate results [12] As such an optimal value for  $u$  can be determined using trial and error. This value was found to be about  $+0.282$ . Substitution of this value yielded a linear delay of  $+0.4455 T_c2\Omega$ . It can be seen that this is only slightly below the previously calculated maximum delay value of  $+0.5T_c2\Omega$ . Having attained a value for  $u$ ,  $v$  was calculated by substitution into (eq. 21). This gives a  $v$  value of  $0.13355$ . Substitution into the defined filter equation (eq. 20), resulted in a transfer function representative of the filter that would represent the linear component of chromatic dispersion:

$$H_{lin}(z) = \frac{(-0.038 - j0.135)z + 0.282}{(1 + j0.282)z - 0.135} \quad (eq. 23)$$

With a filter equation determined for the first term of (eq. 8), another filter was required to represent the parabolic dispersion component represented by the term  $\frac{L}{2} \beta'''(\omega_0) \Omega^2$ . Again a

filter representing this equation was found [15]. This defines the required filter transfer function as:

$$H_{par}(z) = v \frac{z - \frac{1}{v}}{z - v} \quad (eq. 24)$$

Again  $v$  is representative of a real number that characterizes the filters group delay, given by:

$$\tau_{Hpar} = \tau_0 + T_C^3 \frac{v(1+v)}{(1-v)^3} \quad (eq. 25)$$

Here  $\tau_0$  can also be negated on account of its irrelevance to chromatic dispersion. Thus a plot of  $v(1+v)/(1-v)$  as a function of  $v$  could be used to ascertain a maximum value for  $v$ . This led to a  $v$  value of  $1/8$  and a maximum delay value of  $(T_C^{3/8})\Omega^2$ . This  $v$  value was then substituted into equation (eq. 23) to give the transfer function for the parabolic component of chromatic dispersion. Using Simulink, the total chromatic dispersion could be represented by cascading the two filter designs. This was done using another subsystem defined as  $L_2$  and the digital filter design tool block set.

The performance of this filter compared to an ideal filter design was tested using Matlab. A transcript of this process is included in the appendices. It was found that the filter performed well over the majority of the Nyquist bandwidth. Some discrepancies occurred at higher frequencies between the design and ideal case. In this paper this is not considered severe enough to warrant higher order filter implementation on account of the increased processing power required in such an implementation. A higher order filter would be used to enhance the accuracy of any linear dispersion effects.

### 3.13 PMD as a Filter

The other linear cause of pulse broadening, PMD, is caused by fiber birefringence. As previously mentioned birefringence stems from small imperfections in a fiber's symmetry. Thus if a fiber input pulse excites both polarization modes within the fiber dispersion will result. This is a major consideration in modern optical systems. As such the PMD is taken into account in the split step through the linear operator  $L_1^{1/2}$ . The effects of PMD can be modeled by propagating the optical signal through an all pass filter. This is similar to the method employed for the linear chromatic dispersion operator,  $L_2^{1/2}$ . An all pass filter generating the required effects is given by:

$$H_p(z) = z^{-k} \quad (\text{eq. 26})$$

Where  $k$  is a real number representing the number of time samples. The total delay given by the filter can be given by:

$$\tau_p = kT_c \quad (\text{eq. 27})$$

where  $T_c$  is the sampling rate of the input signal. Given this information one simply determines the number of samples occurring over the course of an optical pulse and substitutes for  $k$  in (eq. 26). This gives a filter function that can be implemented using the discrete filter design block.

$$H_{PMD}(z) = z^{-1} \quad (\text{eq. 28})$$

### 3.14 Non-Linear Operator

The parameter  $N$  is representative of a number of non-linear factors. It is reasonable to assume that the nonlinear operator  $N$  is a lumped parameter modeled to take into account the effects of Rayleigh, Brillouin and Raman scattering.[16]. To incorporate these factors one first needs to determine the non-linear threshold. In essence this is a level of power above which the effects of non-linearities need consideration. To include such effects in the simulator the optimum pulse power must be determined. This value will provide the important threshold value above which non-linearities are noticeable.[16]. The pulse power being readily defined as:

$$P_{TH} = \frac{|\beta_2|}{\gamma T_0^2} \quad (eq. 29)$$

Simulations show that non-linearity becomes a relevant contributor to pulse distortion when the laser power is one tenth that of the limiting power defined above as defined by:

$$P_{olaser} \geq \frac{1}{10} P_{TH} \quad (eq. 30)$$

This condition is based upon an analysis of induced errors. It has been demonstrated that laser powers not meeting the above condition induce an error below  $10^{-4}$  when non-linearities are not considered [16]. Leading this to become an accepted level at which non-linearities should be considered. To incorporate any non-linear effects a nonlinear parameter, N, is defined. This parameter acts as a multiplier value dependant upon the injected laser power as defined by [15]:

$$N_2 = \gamma P_0 L D \quad (eq. 31)$$

Where the non-linear parameter,  $\gamma$ , is representative of non-linearities present in a length of fiber.

This parameter is readily defined as [11]

$$\gamma = \frac{2\pi n_2}{\lambda A_{eff}} \quad (eq. 32)$$

where  $n_2$  is the non-linear index coefficient, typically  $10^{-20} \text{m}^2/\text{W}$  for single mode silica fiber.

Where  $\lambda$  represents the operating wavelength and  $A_{eff}$  is the effective area of the fiber. To this end the effective area is calculated using:

$$A_{eff} = \pi r_0^2 \quad (eq. 33)$$

where  $r_0$  is the fiber spot size, given for the Corning SMF-28 as  $4.1 \mu\text{m}$ . This yields an effective area of  $52.81 \mu\text{m}^2$ .

Both the dispersion length,  $L_D$  and the threshold power level are dependant on the value of the dispersion coefficient,  $\beta_2$ . Thus  $\beta_2$  can be calculated using the dispersion relationship:

$$D = \frac{-2\pi c}{\lambda^2} \beta_2 \quad (\text{eq. 34})$$

where the dispersion value.. Substituting and solving gives a  $\beta_2$  value of  $-2.167 \times 10^{-26}$ . It is important to remember the importance of the sign of this value as it represents the direction in which pulse dispersion occurs. Thus any attempt to compensate for dispersion effects must be oppositely signed. Having defined the dependant variables one can proceed to determine the value of N. First gamma was determined using equation (eq. 21) yielding a value of  $7.677 \times 10^{-4} \text{ m}^{-1} \text{ W}^{-1}$ .

Similarly the dispersion length  $L_D$  was found from:

$$L_D = \frac{T_0^2}{|\beta_2|} \quad (\text{eq. 35})$$

To represents the width of the data pulse in seconds. For a 10 ps pulse the dispersion length was found to be about 4615 m. Finally the threshold power,  $P_{TH}$ , is determined using

$$P_{TH} = \frac{|\beta_2|}{\gamma T_0^2} \quad (\text{eq. 36})$$

and estimated about 282.3mW. Thus any laser power greater than 28.2mW would require non-linearity effects to be considered. This was implemented in the simulator by conditionally initializing the value of N. Thus a power greater then the threshold power would cause N to be defined using:

$$N = \sqrt{\gamma P_0 L_D} \quad (\text{eq. 37})$$

Power levels below the threshold would define N as 1 causing non-linear effects to be negligible.

When modeled in Simulink, the non-linear effects are minimal at low power levels, such as single channel systems. Conversely, high power systems will be greatly affected by non-linearities. The challenge in modeling such effects is the need to know a pulse's peak power. For the purposes of this simulation a worst case scenario is considered using the peak energy level of a pulse at a given power injection. This is performed through the use of a Fast Fourier Transform. The input signal is passed into an FFT so as to determine the peak pulse power. This then allows the value of  $N$  to be determined which is in turn multiplied by the input signal in its FFT form. The effects of  $N$  are represented in the optical simulator by the non-linear sub-system,  $N$  incorporated into the fiber propagation subsystem. For simplicity this subsystem is color coded in pink and represented in Figure 5.

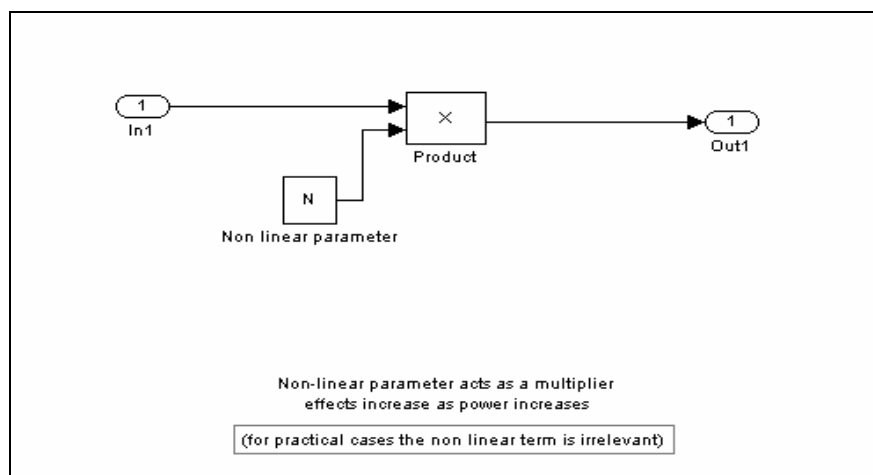


*Figure 5: Non-linear effects model*

It was expected that increasing the power to the data pulse would result in increased dispersion to the signal. However it is important to remember that non-linearities are small in a silica fiber. The effects of the non-linear operator on different power pulses could be monitored. High power pulses should suffer more severe distortion than their low power counterparts in accordance with non-linear effects depending on peak pulse power.

The next section describes the means to run the Simulink optical simulator. Also included are various results and tests attained from the simulator. The biggest advantage of the Simulink optical simulator is its versatility. As such these results are by no means exhaustive. Rather they represent the initial findings of a system that can be expanded to give increasingly detailed results.

#### **4 The Simulator and a Case Study**

The Simulink optical simulator was deliberately designed so as to be as straightforward and easy to operate as possible. The simulator consists of two major components, the initialization file, `initialisation.m`, and the actual simulator itself, `optical simulator.mdl`. To run a simulation, access Matlab 6.5. Open the initialization file from its stored disk, using `file`, then `open`, as per normal. This will bring the Matlab coded initialization file on screen. This file allows the user to define all variables pertaining to the optical simulator. The user is free to modify any value within this file. The file has been commented so as to instruct the user and future designers of the simulators operation. This said, it is likely the user will only modify one or two parameters at any given time. To this end the parameters have been broken into separate fields. More regularly changed parameters being included at the top of the file. The second field of parameters contains those variables pertaining to specific optical fibers. The default values are those of an SMF-28 Corning optical fiber, as defined by the relevant data sheet. These values should only be changed for simulation of different fibers. The remaining file contains values and calculations needed to initialize the optical simulator. It is unlikely these will need to be altered. For a more detailed breakdown of the initialization file refer to the `readme.txt` document included on the simulator disk.

To run a simulation, enter the required parameter values. Then from the debug menu select, `save and run`. This run the file and load the relevant values into both the Matlab workspace and the

Simulink simulator. The simulator should also open in the Simulink workspace. To analyze the initialized system, simply press the run button on the Simulink toolbar. This commences the simulation and automatically opens relevant scopes. All data is also loaded into the Matlab workspace during execution. At the conclusion of the simulation this data can be separately analyzed and considered within the standard Matlab program if desired.

To increase user control and understanding numerous scope and output devices have been incorporated into the simulator. Blue coloring distinguishes these blocksets from the model's data path. Double clicking on the various scope devices will open the scopes output screen. The inclusion of spectrum scopes, eye diagrams and similar tools enhance the simulator's versatility by providing the user with multiple output forms. Any one or all of these may be employed to analyse an optical system. Furthermore the inclusion of scopes throughout the simulator allows the user to better monitor the simulators operation and ensure expected simulator behavior. This presents the user with greater confidence in attained results. Attained results are presented with respect to the simulation time. Thus time values read from results would be directly applicable to practical systems.

To demonstrate the operation of the Simulink optical simulator an example and the consequential results is incorporated. This provides the user with an example that can be followed when employing the optical simulator. The example assumes the following system parameters defined using the initialisation.m file as shown in Figure 6 and listed in the Appendix.

These parameters were loaded using the run command in the debug menu. This resulted in the Matlab platform initializing the values and opening the Simulink optical simulator

*%standard system parameters*

*bit rate=25\*10<sup>9</sup>*

*P<sub>0</sub>=50*

*%bit rate in Gb/s*

*%laser pulse power in mW (0.1 to 10 mW)*

$\text{deltaz} = 0.5$	<i>%split step length in km</i>
$L = 10$	<i>%length of fiber in kilometers</i>
$\text{bitnum} = 16$	<i>%number of bits in data string,</i>
$\text{lamda} = 1.55 \cdot 10^{-6}$	<i>%operating wavelength in m</i>
$T_p = 10 \cdot 10^{-12}$	<i>%pulse time(width) in seconds</i>

Figure 6 : Initializing the simulator

The run button was then used to start the simulation and the output of the various scopes noted.

Figure 7 gives a sample screen shot as the simulator commences operation.

Two cases have been included in this report. One of these includes sufficient channel power to induce non-linear effects. The second does not. This allows comparative conclusions to be drawn about the non-linear effects. Other cases were modeled to test the system, however for the sake of brevity only these two cases have been included in this work.

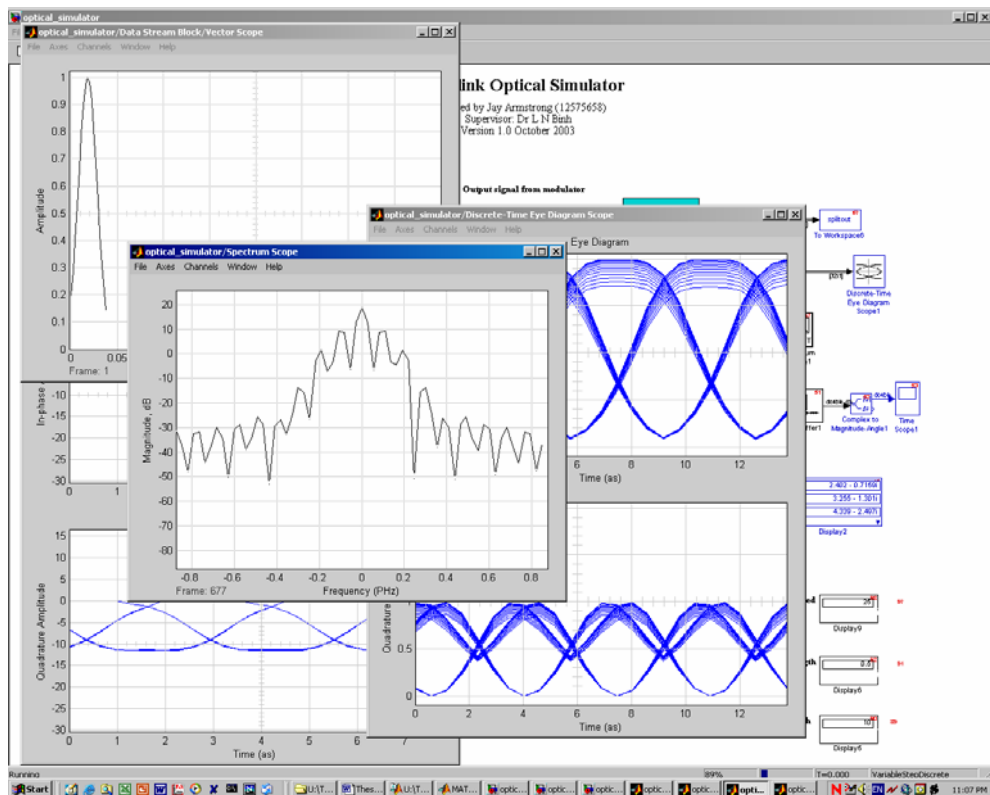


Figure 7: Sample screen shot of the SIMULINK simulator

To include non-linear effects a power input of 50mW was injected as the peak laser power input. This value was above the threshold condition, 28.2mW, and resulted in an N parameter of (add N value here). Such a system could be representative of a multiple channel optical transmission system in which power levels as high as 100mW can be employed. For the low power simulation a 5mW channel power was used. This would result in negligible non-linear effects resulting in an N value of 1. This could represent a single channel or low channel count system. The attained plots for these cases are shown in Figure 8.

The plots illustrate a number of key factors that occur when propagating an optical signal. In particular the eye diagram can be used to determine the bit error rate. The spectrum scope plots clearly illustrate the power of the carrier and its associated data sidebands. For comparative purposes the same data stream was used in both the high and low power cases in order to examine the non-linear effects on pulse distortion.

The advantage of the simulator is undoubtedly its versatility. One need not plot all this data every time the simulation is run. Rather one can select the data most of use, such as the eye diagram. This adds to the systems versatility by ensuring that only data relevant to the user is displayed.

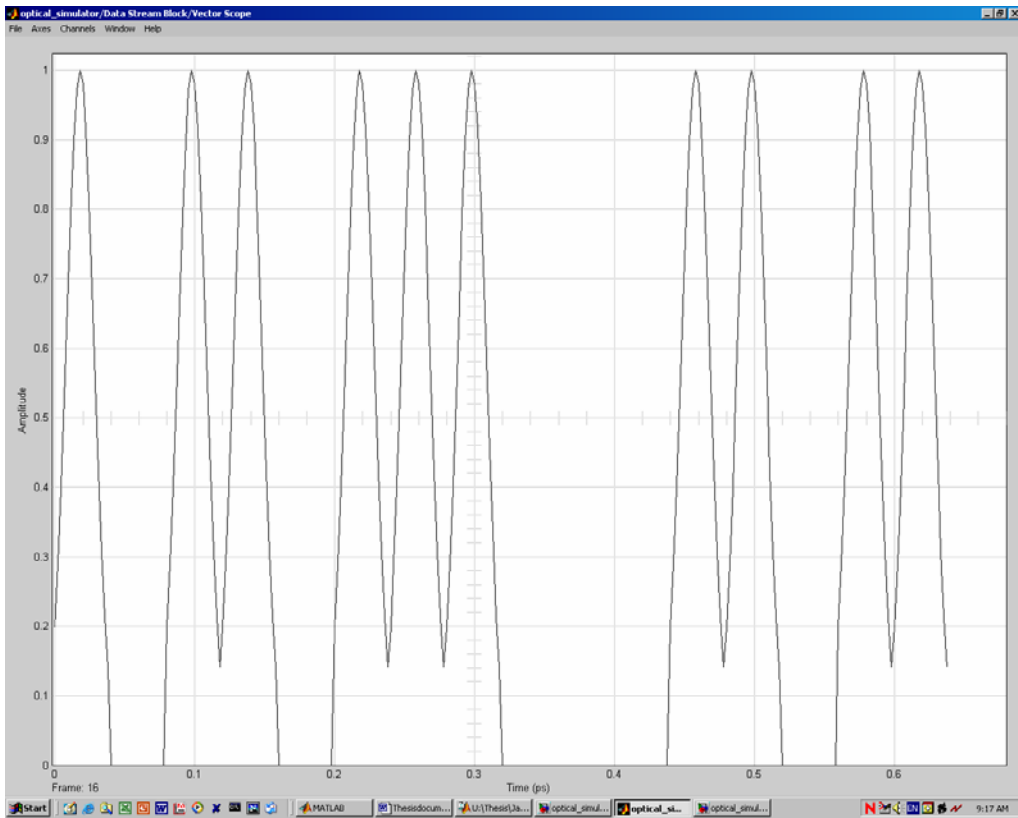


Figure 8(a) *Gaussian-shape pulse train*

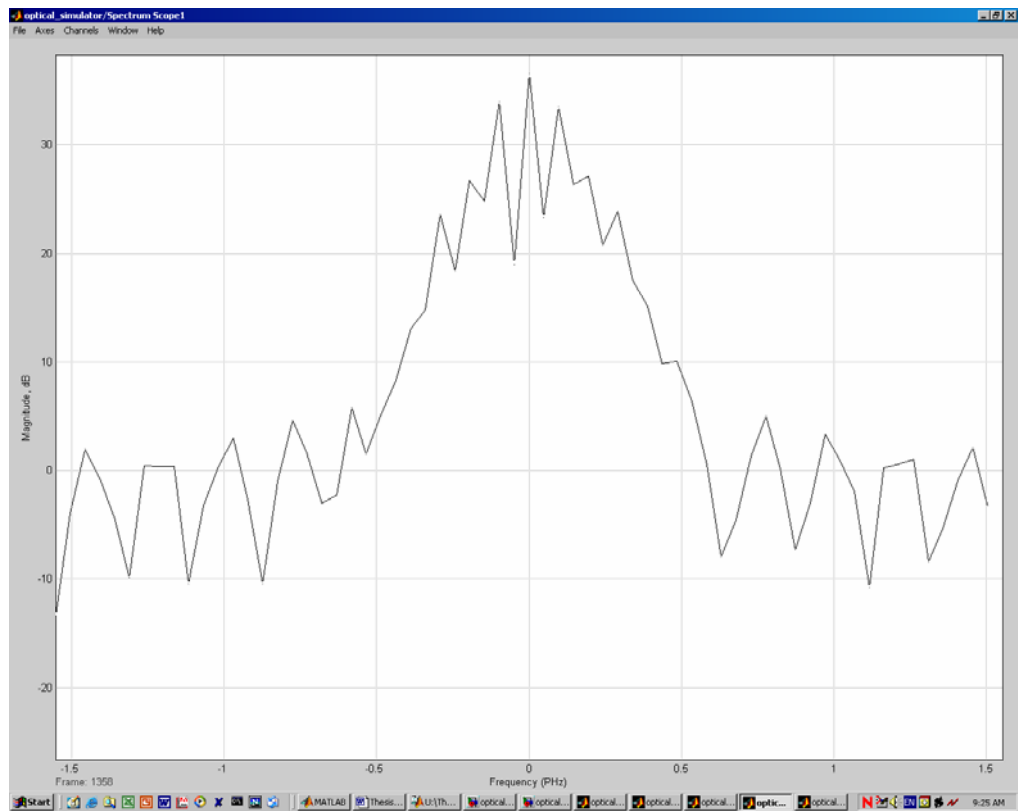
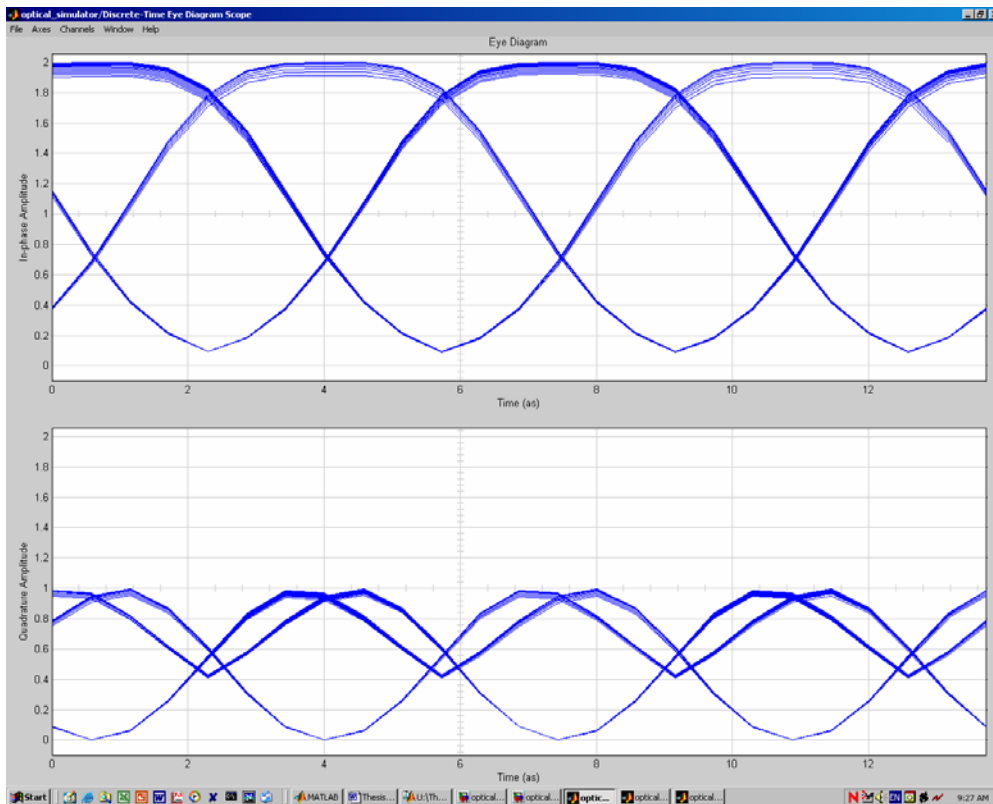


Figure 8(b) *Modulator output spectrum*Figure 8(c) *Eye diagram at modulator output*

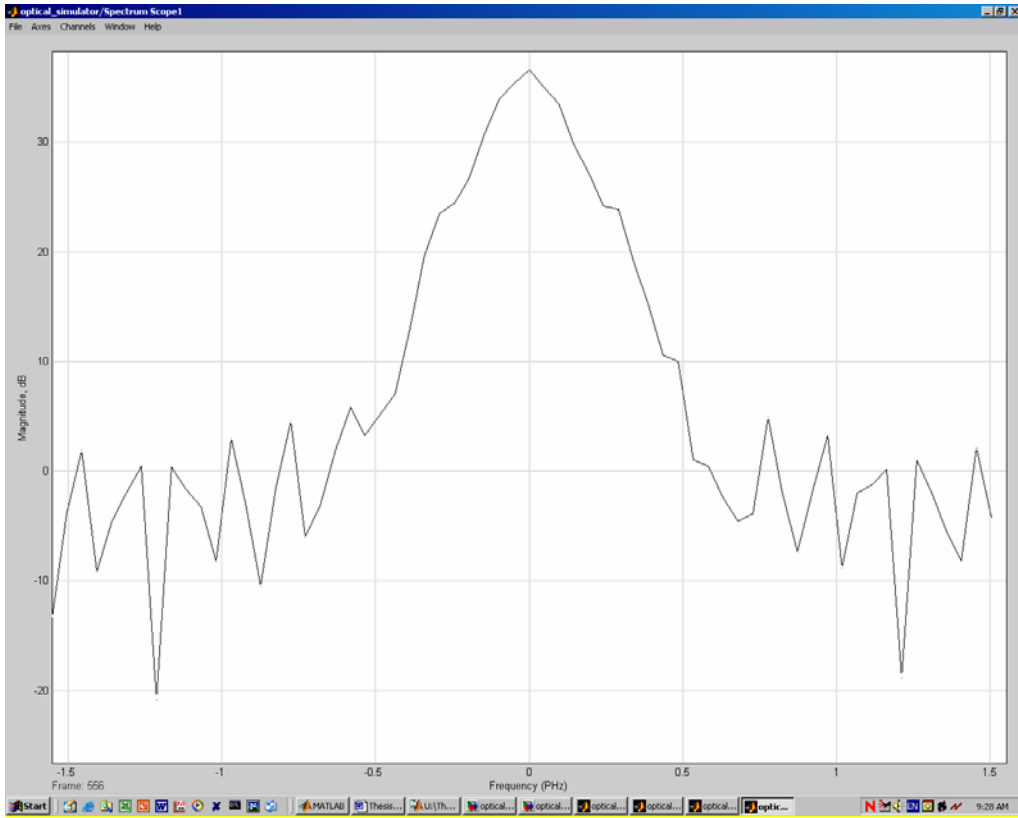


Figure 8(d) *Propagated output spectrum*

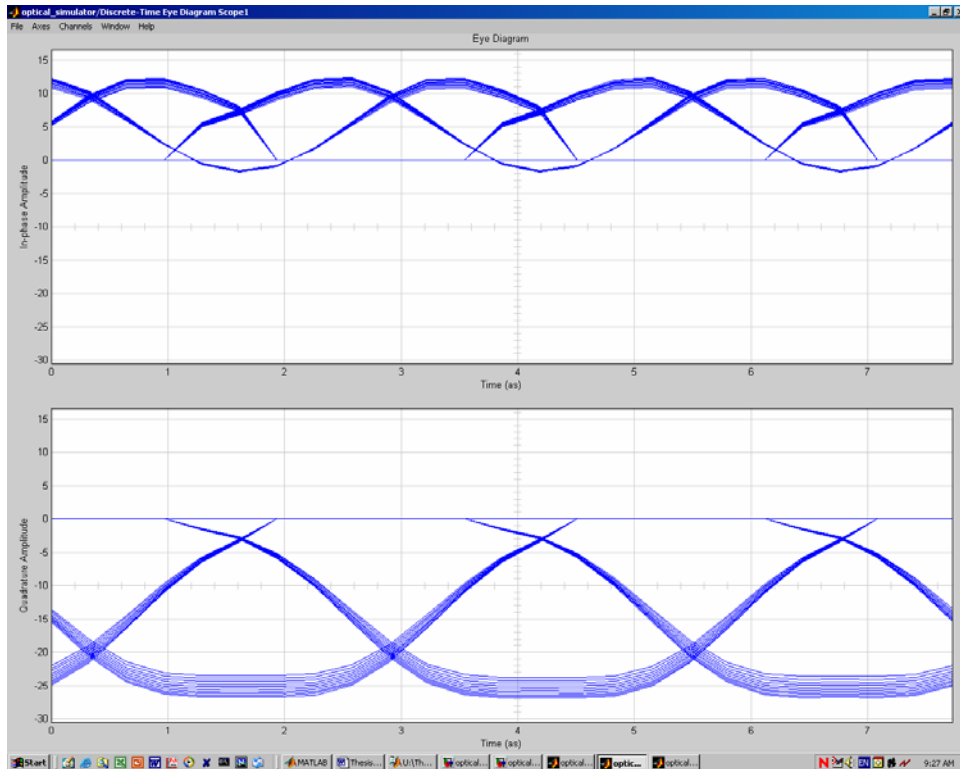
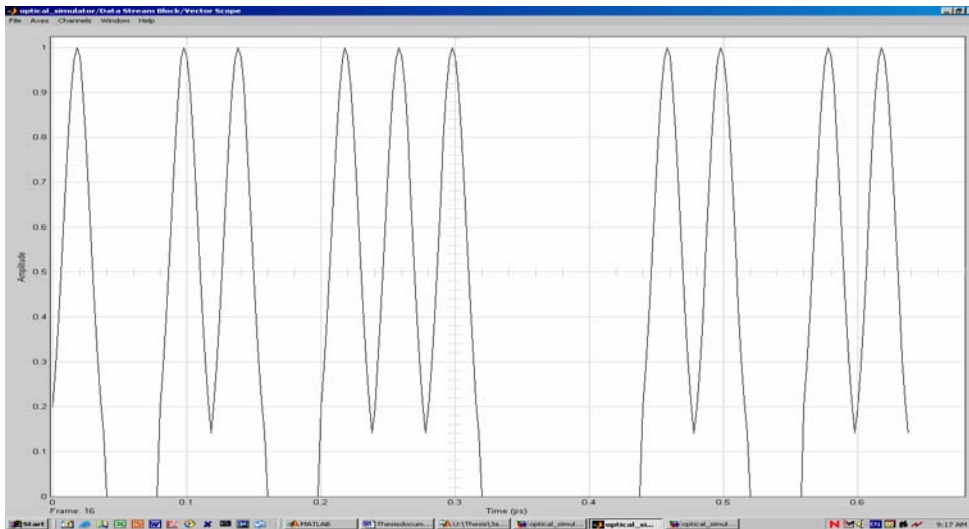
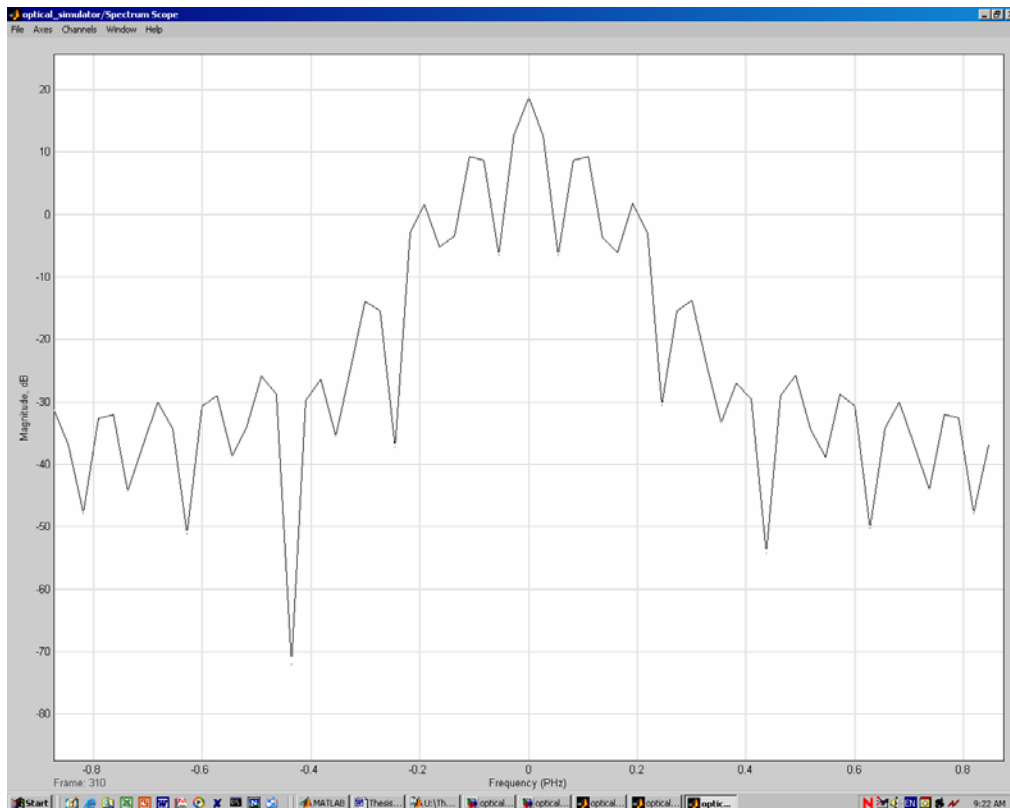


Figure 8(e) *Propagating output eye diagram*Figure 8: (a)-(e) 5mW simulation – Non-linear effects negligible,  $N=1$ Figure 9(a) *Shaped Gaussian pulse*Figure 9(b) *Modulator output spectrum*

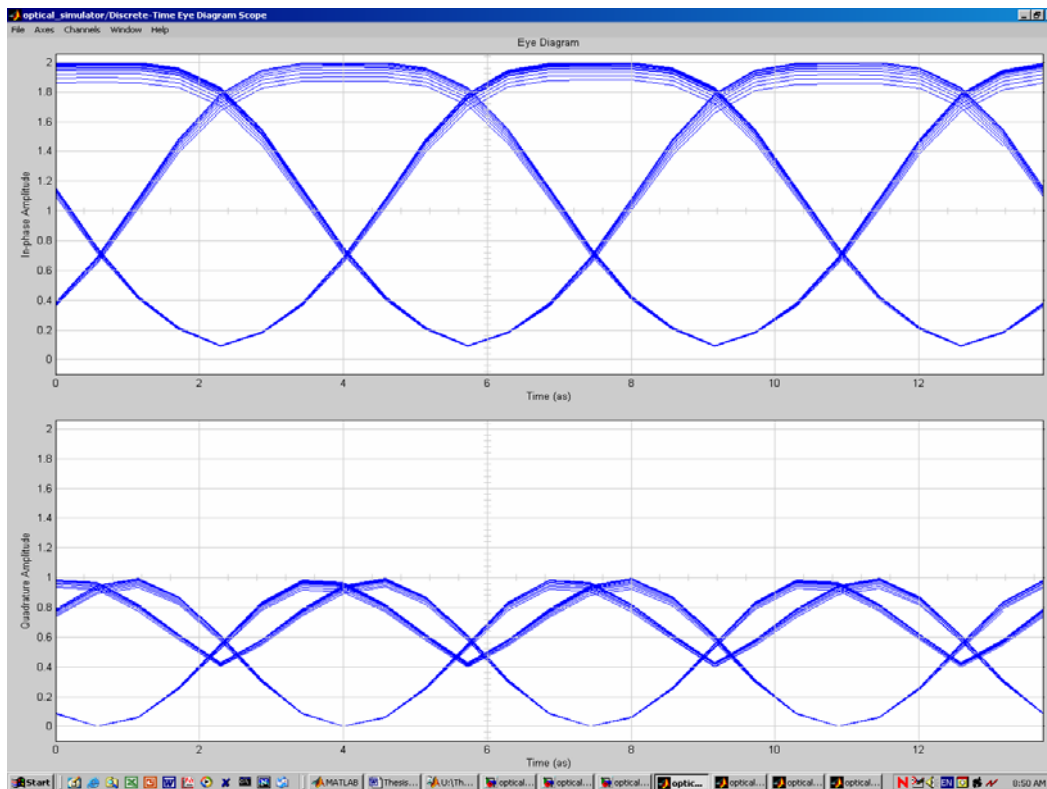


Figure 9(c) Modulator output eye diagram

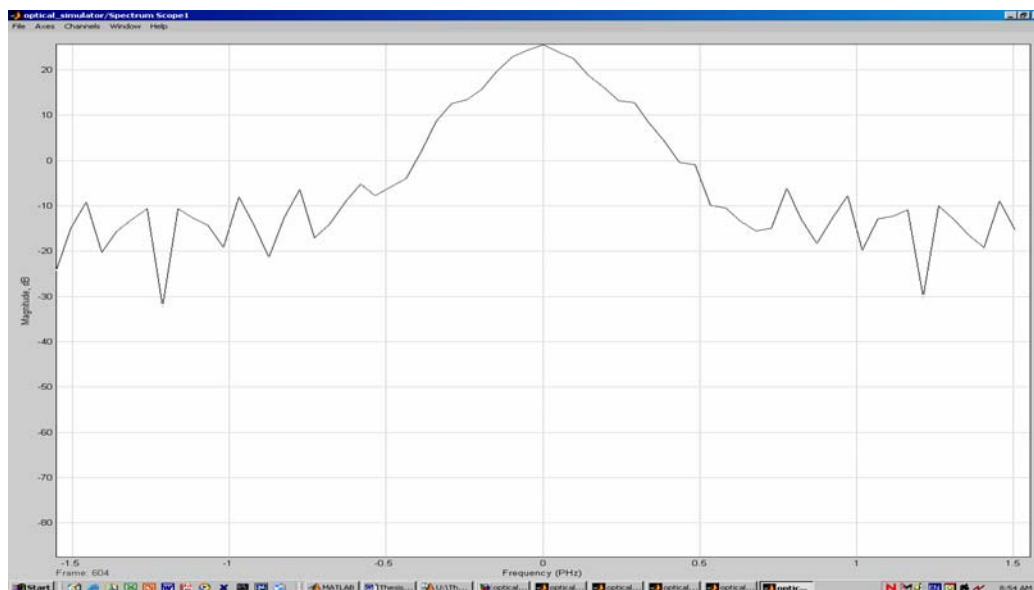


Figure 9(d) Propagated output spectrum

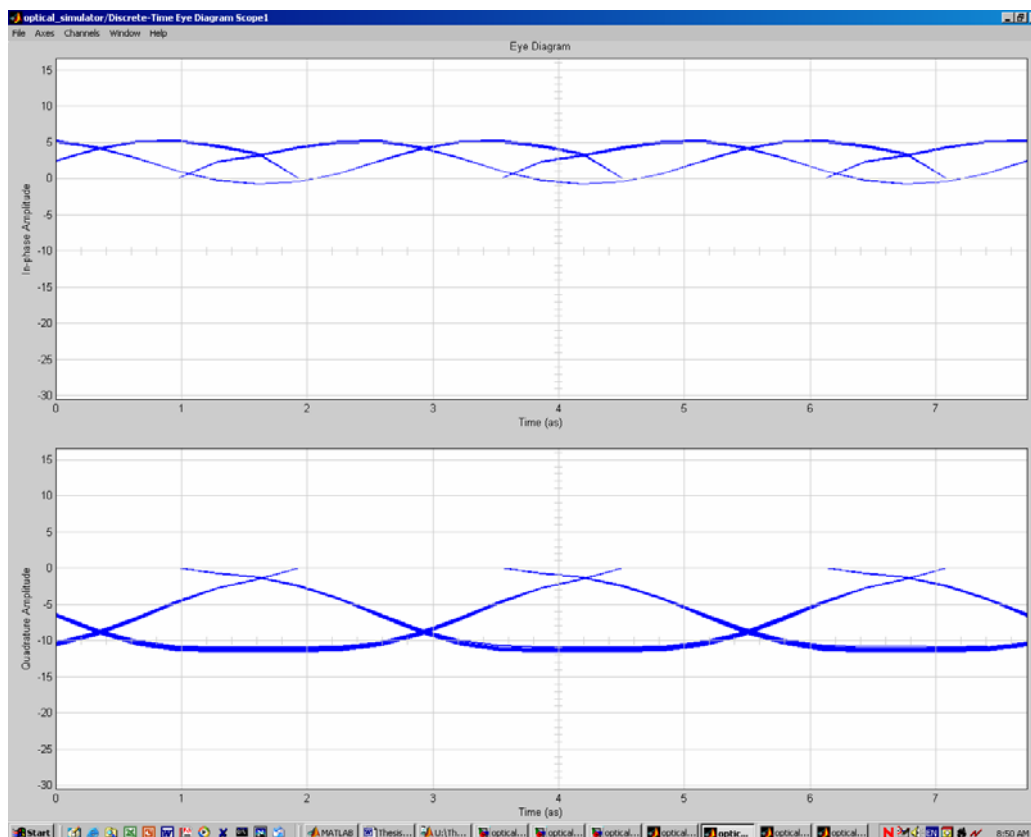


Figure 9(e) *Propagated output eye diagram*

Figure 9: 50mW case – Non-linear effects,  $N=0.429$

A number of considerations can be drawn from the two case studies. Most importantly, the effects of propagating an optical signal along a single step of fiber are clearly illustrated. A comparison of the modulator output and the fiber output clearly shows the simulated dispersion effects caused by the fiber. Figure 10 shows the modulator and fiber output plots attained for the 5mW laser/channel simulation.

The left hand side of Figure 10 shows the undistorted modulated eye diagram attained at the output of the modulator. However, after propagation through the fiber, shown by the right hand eye-diagram, the pulse is clearly broadened in accordance with the effects of GVD and PMD. The clean eye opening demonstrated at the modulator output has lost some of its shape after propagation through the fiber length. At the high power results, the pulse distortions due to the

non-linear effects are clearly shown. The GVD and PMD are still clearly evident. The pulses have not only broadened but the eyes have also been partially closed. This would reduce a systems margin for error and likely increase a systems bit error rate once a receiver was incorporated.

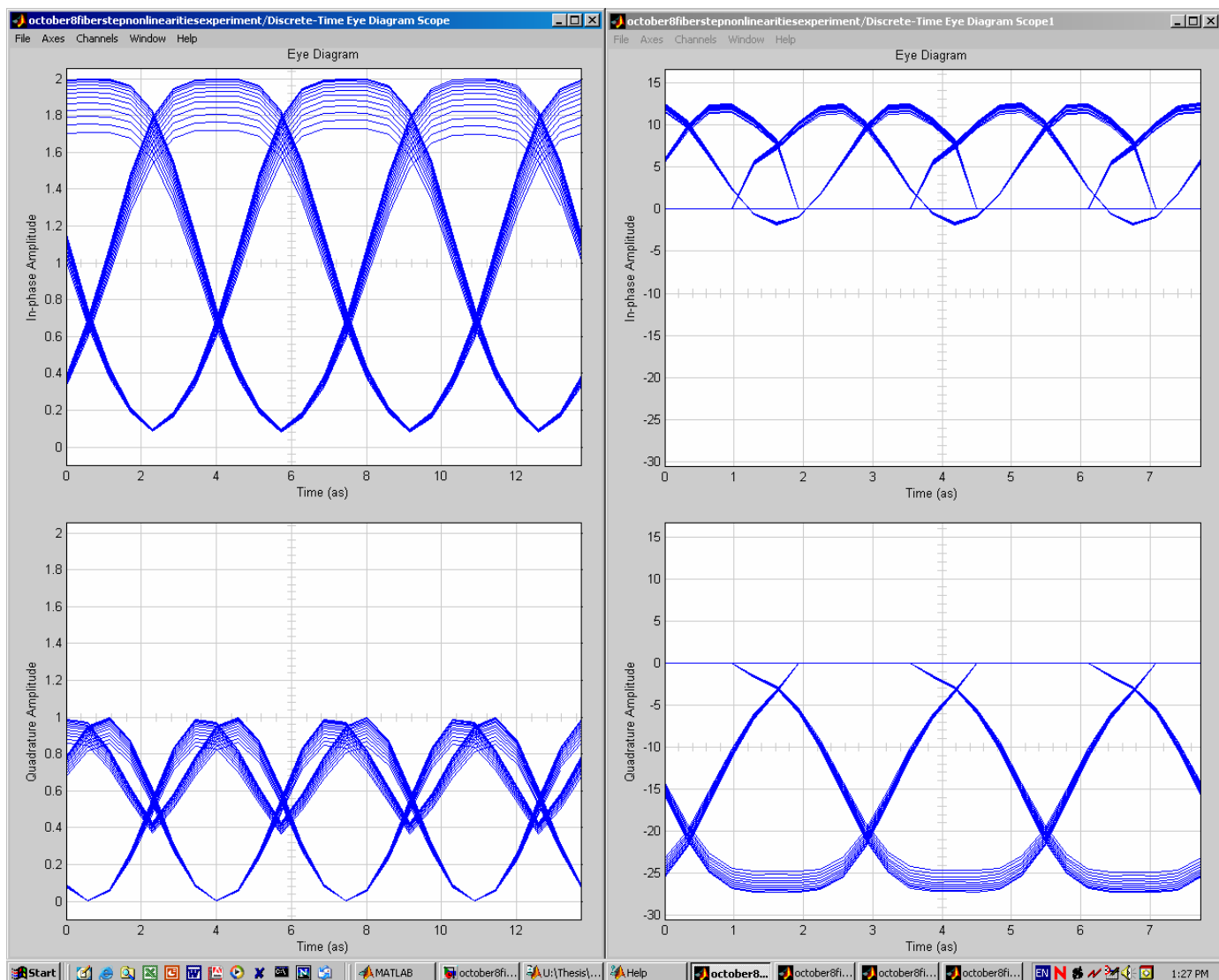


Figure 10: Comparison of modulator output and fiber outputs for an input power of 5mW

## 5 CONCLUDING REMARKS

Primarily a simulink optical transmission system and its various photonic components has been established. Initial research focused upon the various technologies used such system. The operation of these technologies has been deeply explored and in some cases developed for The SIMULINK Optical Simulator - Fibre Optic Transmission Systems

further use. Negative dispersion usually occurs as a result of signal propagation through a modulator, optical fiber or as a result of the optical carrier. Deliberately inducing a positive chirp via the external modulator model, either through the tuning of the optical carrier or a phase shift in the modulator may allow the limitations of chirp to be overcome.

To this end a fiber optic communication system simulation platform is developed. Based in the Matlab subsidiary program, Simulink, this program can simplify the simulation process of modern optical transmission systems. Simulink can simulate the fiber propagation through the use of the split step method without difficulties. The dispersion effects of GVD, PMD and non-linear factors were modeled independently over a short length of fiber. This allowed the individual contribution of each effect to be analyzed. Also simulated were the operations of the Mach-Zehnder Interferometric Modulator (MZIM) and its necessary components, the carrier and the data stream. More importantly, the developed simulator provides a platform upon which a powerful simulation tool can be developed.

Future works will aim to incorporate a greater number of optical components into the simulator, further enhancing the uses of the simulator. The modeling of each effect over a short fiber length can then be looped and iteratively calculated to model the performance of long haul optical transmission systems. It is hoped that the optical simulator will provide the base framework upon which optical transmission systems up to three thousand kilometers can be simulated.

This paper has outlined the flexibility of simulation techniques. Simulink provides a simple means to upgrade the existing model. Another designer need not sift through pages of code and variables in an attempt to understand the systems operation. Furthermore, a desire to incorporate additional components, such as amplifiers, is relatively easily performed. A designed subset modeling any given effect is simply placed within the propagation path. That means simulations can be developed for numerous optical components and included or excluded at the user's

discretion. In essence, an entire library of components could be developed for use. Various dispersion compensation techniques, optical amplifiers and various receiver technologies will also be modeled. A great deal of insight may also be gathered on long haul transmission systems. Including all relevant sub-systems and looping data back through the split step would perform simulations for any given length of fiber.

## 6 References

- [1] Agrawal, G.P., Fiber-Optic Communication Systems 2nd Ed, J. Wiley and Sons, Sydney, 1997.
- [2] Allard, F.C., Fiber Optics Handbook, McGraw-Hill Publishing Company, New York, 1989.
- [3] Bogner, R.E. and Constantinides, A.G., Introduction to Digital Filtering, John Wiley and Sons, Sydney, 1975.
- [4] Kreyszig, E., Advanced Engineering Mathematics 7th Ed, John Wiley and Sons, New York, 1993.
- [5] Proakis, J.G., Digital Communications 3rd Ed, McGraw-Hill Publishing Company, New York, 1995.
- [6] Baher, H and Beneat, J, "Design of Analog and Digital Transmission Filters", IEEE Trans. Circuits Syst., vol 40, no 7, July 1993.
- [7] Carena, A. et al, "A Time-Domain Optical Transmission System Simulation Package Accounting for Nonlinear and Polarization-Related Effects in Fiber", IEEE J. Sel. Areas Comm., vol 15, No. 4, May 1997, pp751-764.
- [8] Courjal, N et al, "LiNbO<sub>3</sub> Mach-Zehnder Modulator With Chirp Adjusted by Ferroelectric Domain Inversion", IEEE Photonics Tech. Lett., vol 14, no 11, Nov. 2002, pp1509-1511.
- [9] Jackson, M K et al, "Optically Linearized Modulators: Chirp Control for Low Distortion Analog Transmission", J.Lightw.Tech., vol 15, No. 8, Aug. 1997, pp1538-1545.
- [10] Jeong, J and Park, Y K, "Accurate determination of transient chirp parameter in high speed digital lightwave transmitters", Elect. Lett., vol 33, no 7, 27th March 1997.
- [11] Kim, H and Gnauck, A H, "Chirp Characteristics of Dual-Drive Mach-Zehnder Modulator With A Finite DC Extinction Ratio", IEEE Photonics Tech.Lett., vol 14, no 3, March 2002, pp298-300

[12] Koyama, F., “Frequency Chirping in External Modulators”, J. Lightw. Tech., vol 6, No. 1, Jan. 1998, pp87-93.

[13] Laverdiere, C. et al, “A new method for measuring time-resolved frequency chirp of high bit rate sources”, IEEE Photonics Tech. Lett., vol 15, no 3, March 2003, pp446-448.

[14] Saunders, R A et al, “Wideband chirp measurement technique for high bit rate sources”, Elect. Lett., vol 30, no.16, Aug. 1994, pp1336-1338.

[15] Xie Y at al., “System Performance Degradation due to Nonlinear Signal Distortion in Spectral Inverter”, J. Optical Comm., vol 19, no 4, 1998

[16] Binh, L.N., ECE4405: Optical Communication Systems Notes, Monash University, 2002

[17] Selliah, A., “Simulation of Polarisation Mode Dispersion Effects in A DWDM System: a time domain approach”, Monash University Thesis, 2001.

## 7 APPENDIX

```

%%%%%%%%%%%%%%%%%%%%%%%%%%%%%%%%%%%%%%%%%%%%%%%%%%%%%%%%%%%%%%%%%%%%%%%%
%
% Simulink Optical Simulator initialisation
%
%%%%%%%%%%%%%%%%%%%%%%%%%%%%%%%%%%%%%%%%%%%%%%%%%%%%%%%%%%%%%%%%%%%%%%%%

```

```

%before running simulator define the standard system parameters
%then go to debug menu and select run, simulink model will automatically
%open, press the run button in simulink to begin the simulation

```

```

%standard system parameters
bitrate=25*10^9           %bitrate in gb/s
P0=50                    %laser pulse power in mW (0.1 to 10 mW)
deltaz=0.5               %split step length in km
L=10                     %length of fiber in kilometers
bitnum=16                %number of bits in data string,
lamda=1.55*10^-6         %operating wavelength in m
Tp= 10*10^-12           %pulse time(width) in seconds

```

```

%optional parameters varied for different fiber parameters
r0=4.1*10^-6             %fiber spot size in m^2
n2=10^-20                %non-linear index coefficient in m^2/W
D=17                    %dispersion parameter in ps/nm.km
speedlight=3*10^8        %speed of light in m/s

```

```

%%%%%%%%%%%%%%%%%%%%%%%%%%%%%%%%%%%%%%%%%%%%%%%%%%%%%%%%%%%%%%%%%%%%%%%%
%
%system functions, no need to vary these values
%%%%%%%%%%%%%%%%%%%%%%%%%%%%%%%%%%%%%%%%%%%%%%%%%%%%%%%%%%%%%%%%%%%%%%%%

```

```

time=(bitnum-1)*(1/bitrate) %simulation time for desired bit string
I0=(P0+3.31)/0.133          %carrier current/amplitude

```

```

iterations=L/deltaz

```

```

%defining carrier and pulse waveforms
tc=0:5.155*10^-17:5.10345*10^-15      %define one period of carrier
tc=tc'                                %convert tc to vertical matrix
fc=1.94*10^14                          %define the frequency of the carrier in Hz
c=10*sin(2*pi*fc*tc)                   %define carrier sinusoid
carrier=[tc c]

m=sin(2*pi*fc*tc+pi)                   %modulating waveform

tg=5*10^-9:0.55*10^-9:5*10^-9          %define gaussian pulse period
t0=3.5*10^-9                            %define standard deviation of gaussian pulse
y=exp(-(tg/t0).^2)                       % define gaussian pulse waveform
gauss=[y]

%need to determine whether non linear effects required

Aeff=pi*(r0)^2                           %calculate fiber effective area
beta2=-((D*10^-6)*(lamda^2))/(-2*pi*speedlight)%calculate dispersion coefficient
gamma=(2*pi*n2)/(lamda*Aeff)              %calculate nonlinear coefficient
Ld=(Tp^2)/(abs(beta2))                    %calculate the dispersion length
Preq=(abs(beta2))/(gamma*(Tp^2))          %power required to generate pulse in Watts
P0=P0*10^-3

if P0<(Preq/10)                           %check non linearity limit and determine non linear parameter
    N=1                                    %if fiber power < pulse required per pulse non-linearities negligible
else
    N=(gamma*Ld*P0)^0.5                    %If fiber power >= pulse required incorporate non linear effects
end

open('E: \Optical Simulator\optical_simulator.mdl')

%open simulator model in simulink, may need to alter path if not on
%installation disk

%%%%%%%%%%%%%%end initialisation file%%%%%%%%%%%%%%

```